

# A new experimental approach to detect long-range conformational changes transmitted between the membrane and cytosolic domains of LmrA, a bacterial multidrug transporter

Catherine Vigano<sup>a,1,\*</sup>, Vinciane Grimard<sup>a,1</sup>, Abelardo Margolles<sup>b,2</sup>, Erik Goormaghtigh<sup>a,3</sup>, Hendrik W. van Veen<sup>c</sup>, Wil N. Konings<sup>b</sup>, Jean-Marie Ruyschaert<sup>a</sup>

<sup>a</sup>Service de Structure et Fonction des Membranes Biologiques (SFMB), Université Libre de Bruxelles, P.O. Box 206/2, Bd du Triomphe, B1050 Brussels, Belgium

<sup>b</sup>Department of Microbiology, Groningen Biomolecular Sciences and Biotechnology Institute, University of Groningen, 9751 NN Haren, The Netherlands

<sup>c</sup>Department of Pharmacology, University of Cambridge, Cambridge CB2 1QJ, UK

Received 29 June 2002; revised 6 September 2002; accepted 6 September 2002

First published online 1 October 2002

Edited by Gianni Cesareni

**Abstract** LmrA confers multidrug resistance to *Lactococcus lactis* by mediating the extrusion of antibiotics, out of the bacterial membrane, using the energy derived from ATP hydrolysis. Cooperation between the cytosolic and membrane-embedded domains plays a crucial role in regulating the transport ATPase cycle of this protein. In order to demonstrate the existence of a structural coupling required for the cross-talk between drug transport and ATP hydrolysis, we studied specifically the dynamic changes occurring in the membrane-embedded and cytosolic domains of LmrA by combining infrared linear dichroic spectrum measurements in the course of H/D exchange with Trp fluorescence quenching by a water-soluble attenuator. This new experimental approach, which is of general interest in the study of membrane proteins, detects long-range conformational changes, transmitted between the membrane-embedded and cytosolic regions of LmrA. On the one hand, nucleotide binding and hydrolysis in the cytosolic nucleotide binding domain cause a repacking of the transmembrane helices. On the other hand, drug binding to the transmembrane helices affects both the structure of the cytosolic regions and the ATPase activity of the nucleotide binding domain.

© 2002 Federation of European Biochemical Societies. Published by Elsevier Science B.V. All rights reserved.

**Key words:** Multidrug resistance; LmrA; Infrared spectroscopy; Tryptophan fluorescence; Membrane domain; Conformational change

## 1. Introduction

Multidrug resistance is often mediated by membrane transport proteins and results in the inefficiency of cancer and infectious disease treatments [1,2]. Some of these proteins that transport a broad spectrum of structurally unrelated cytotoxic drugs act as ATP-driven efflux pumps. In cancer cells, multidrug resistance to chemotherapy mainly results in the overexpression of ABC (ATP binding cassette) transporters like Pgp (P-glycoprotein) [3] and MRP (multidrug resistance-associated) proteins [4]. LmrA, from *Lactococcus lactis*, also belongs to the ABC superfamily and its expression results in an increased bacterial resistance to different antibiotics [5]. This protein is a structural and functional homologue of the mammalian Pgp. Indeed, both proteins have a similar drug and modulator specificity [6]. Furthermore, LmrA can even functionally complement Pgp in human fibroblast cells [7].

ABC transporters are composed of four core domains [8]. Two of these domains are hydrophobic and located within the membrane. Hydrophobic models predict that each of these domains contains six  $\alpha$ -helices. Two other domains are hydrophilic and contain the NBDs (nucleotide binding domain) which hydrolyze ATP. Pgp contains these four domains in one polypeptide chain [9,10]. In contrast, LmrA appears to be half a transporter, only containing one hydrophobic and one hydrophilic domain [6]. However, it is functionally active as a homodimer [11]. Pgp and LmrA share a high sequence homology, notably in their NBDs, which is a general property of all ABC transporters. Furthermore, their hydrophobic domains implicated in drug recognition and transport [12,13] also share a high level of homology [6]. The use of polarized infrared spectroscopy demonstrated that the transmembrane segments of LmrA are made of  $\alpha$ -helices oriented perpendicular with respect to the membrane [14]. Three-dimensional crystals of MsbA [15] and BtuCD [16] have confirmed that the helical nature of the membrane-embedded domain is a general characteristic of ABC transporters.

A transport model, based on transport measurements, drug equilibrium determinations and photoaffinity labelling, proposes that LmrA functions by an alternating two-site mechanism [11]. In this model, LmrA passes through two configurations, containing a high-affinity, inside-facing, drug binding

\*Corresponding author. Fax: (32)-2-650 53 82.

E-mail address: cvigano@ulb.ac.be (C. Vigano).

<sup>1</sup> Research Fellows of the National Fund for Scientific Research (Belgium).

<sup>2</sup> Recipient of a TMR fellowship of the EU.

<sup>3</sup> Research Director of the National Fund for Scientific Research (Belgium).

**Abbreviations:** ABC, ATP binding cassette; ATP<sub>γ</sub>S, adenosine-5'-O-(thiotriphosphate); ATR-FTIR, attenuated total reflection Fourier transform infrared; DDM, dodecyl- $\beta$ -D-maltoside; DNR, daunorubicin; MDR, multidrug resistance; MRP, multidrug resistance protein; NBD, nucleotide binding domain; Ni-NTA, Ni<sup>2+</sup>-nitrilotriacetic acid; Pi, inorganic phosphate; Pgp, P-glycoprotein

site and a low-affinity, outside-facing, drug release site and the interconversion of these two configurations is ATP-dependent. A similar mechanism has been proposed for Pgp [17–20]. This model requires the existence of a structural cooperation between the membrane and cytosolic domains leading to the coupling mechanism between the hydrolysis process and the transport of drug. The characterization of such a structural coupling is of clinical interest. Indeed, compounds perturbing interactions between the cytosolic and membrane-embedded domains may interfere with the transport function of LmrA and modulate multidrug resistance phenomena in general.

The main goal of the present study is to investigate whether long-range conformational changes are transmitted between the membrane and cytosolic domains of LmrA and to characterize their nature. For this purpose, we took advantage of two complementary methods to detect specific structural changes occurring in either the membrane-embedded or cytosolic regions of LmrA. On the one hand, Trp fluorescence quenching by acrylamide, an aqueous quencher, was used to observe changes occurring in the cytosolic regions in the presence of drug or during the hydrolysis process. On the other hand, monitoring the infrared linear dichroic spectra in the course of H/D exchange made it possible to focus exclusively on the membrane-embedded  $\alpha$ -helices and to observe how they are affected by ATP/drug binding and ATP hydrolysis. Experiments were carried out in the presence of different ligands in order to characterize structural intermediates involved in the transport process. First, daunorubicin (DNR), a cytotoxic drug well transported by LmrA, was used to identify the structural effect due to drug binding. Second, ATP and its non-hydrolyzable analogue ATP $\gamma$ S (adenosine-5'-O-(thiotriphosphate)) [21] were used to discriminate between the structural effects mediated by ATP hydrolysis and ATP binding respectively.

## 2. Materials and methods

### 2.1. Materials

ATP, ATP $\gamma$ S and DNR were from Sigma. D<sub>2</sub>O was from Merck, Ni-NTA (Ni<sup>2+</sup>-nitrilotriacetic acid) resin from Qiagen, Bio-Beads SM2 from Bio-Rad, polycarbonate filters from Avestin and DDM (dodecyl- $\beta$ -D-maltoside) from Anatrace. *Escherichia coli* lipids and L- $\alpha$ -phosphatidylcholine from egg yolk were purchased from Avanti Polar Lipids.

### 2.2. Bacterial strains and expression vector

*L. lactis* subsp. *lactis* strain NZ9000 was used as a host for the LmrA expression vector used in this work [22]. The pCHL LmrA vector [7] was used in this study after introduction of an *Nco*I site upstream of the hexahistidine tag and an *Xba*I site at the 3' end of LmrA. This plasmid was transformed into *L. lactis* NZ9000 and the transformants were screened by restriction analysis of the plasmids [22].

### 2.3. Purification

The purification of LmrA was carried out essentially as described previously [22]. Briefly, inside-out membrane vesicles, containing overexpressed LmrA, were solubilized in 50 mM potassium phosphate, pH 8, containing 10% (v/v) glycerol, 100 mM NaCl and 1% (w/v) DDM. After 30 min incubation at 4°C, the insoluble material was removed by centrifugation. The supernatant was mixed and incubated for 1 h, at 4°C, with Ni-NTA agarose (approximately 8 mg LmrA/ml resin), which was pre-equilibrated in buffer A (50 mM potassium phosphate, pH 8, 100 mM NaCl, 10% glycerol and 0.05% DDM) plus 10 mM imidazole. The resin was transferred to a Bio-spin column (Bio-Rad) and washed with 20 column volumes of buffer A containing 10 mM imidazole, and subsequently with 40 column volumes of buffer A

(pH 7) plus 40 mM imidazole. The protein was eluted with buffer A, pH 7, supplemented with 150 mM imidazole.

### 2.4. Reconstitution

Liposomes of acetone/ether-washed *E. coli* lipids and L- $\alpha$ -phosphatidylcholine from egg yolk, in a ratio (w/w) of 3:1, were made by dissolving lipids in 50 mM potassium phosphate, pH 7, at a final concentration of 20 mg/ml. Unilamellar liposomes with relatively homogeneous size were prepared by freezing in liquid nitrogen and slow thawing at room temperature followed by extrusion of the liposomes 12 times through a 400-nm polycarbonate filter. The reconstitution of LmrA into liposomes was carried out essentially as described in [22] using a (w/w) protein:lipid ratio of 1/10. The resulting proteoliposomes exhibited ATP-dependent drug transport, inhibited by chemosensitizers [22]. Proteoliposomes were resuspended to a final protein concentration of 1 mg/ml in 3 mM potassium HEPES, pH 7.4.

### 2.5. Attenuated total reflection Fourier transform infrared spectroscopy (ATR-FTIR)

ATR-FTIR spectra were recorded, at room temperature, on a Bruker IFS55 FTIR spectrophotometer equipped with a liquid nitrogen-cooled mercury-cadmium-telluride detector at a nominal resolution of 2 cm<sup>-1</sup>, and encoded every 1 cm<sup>-1</sup>. The spectrophotometer was continuously purged with air dried on a FTIR purge gas generator 75-62 Balston (Maidstone, UK) at a flow rate of 5.8 l/min. The internal reflection element (ATR) was a germanium plate (50 × 20 × 2 mm) with an aperture angle of 45°, yielding 25 internal reflections [23].

**2.5.1. Sample preparation.** The sample contained 20  $\mu$ g of reconstituted LmrA. For measurements in the presence of DNR, 2.5  $\mu$ l of a 2 mM solution was added to the proteoliposomes. In these conditions, the molar ratio of LmrA over DNR is 1/14. For measurements in the presence of MgATP $\gamma$ S or MgATP, 0.5  $\mu$ l of a 3 mM solution was added to reach a molar ratio of LmrA over nucleotides of 1/5. Thin films of oriented multilayers were then obtained by slowly evaporating the sample on one side of the ATR plate, under a stream of nitrogen [24]. It has been shown that after resuspension in 3 mM HEPES pH 7.4, no loss of ATPase activity was observed, confirming that film preparation does not alter the protein conformation and activity. The ATR plate was then sealed in a universal sample holder.

**2.5.2. Orientation of the secondary structures.** The molecular orientation was determined by infrared ATR spectroscopy as previously described [25]. Spectra were recorded with parallel and perpendicular polarized light with respect to the incidence plane. Dichroic spectra were computed by subtracting the perpendicularly polarized spectrum from the parallelly polarized spectrum. The subtraction coefficient was chosen so that the area of the lipid ester band at 1740 cm<sup>-1</sup> equals zero on the dichroic spectrum, in order to take into account the difference in the relative power of the evanescent field for each polarization as described before [25]. An upward deviation on the dichroic spectrum indicates a dipole oriented preferentially near a normal to the ATR plate. Conversely, a downward deviation on the dichroic spectrum indicates a dipole oriented closer to the plane of the ATR plate [23]. The dichroic ratio  $R^{\text{ATR}}$  is defined as the ratio of the amide I area recorded for the parallel polarization ( $A^{\parallel}$ ) and for the perpendicular polarization ( $A^{\perp}$ ):

$$R^{\text{ATR}} = A^{\parallel}/A^{\perp}$$

In ATR, the dichroic ratio for an isotropic sample  $R^{\text{iso}}$  is different from unity and is computed on the basis of the area of the lipid ester band (1762–1700 cm<sup>-1</sup>) [26].

**2.5.3. H/D exchange kinetics of the oriented domain of the protein.** Films containing 20  $\mu$ g of reconstituted LmrA were prepared on a germanium plate as described above. Nitrogen was saturated with D<sub>2</sub>O by bubbling in a series of three vials containing D<sub>2</sub>O. Spectra were recorded with the incident light polarized perpendicular and parallel with respect to the incident plane for each time point of the kinetics. The dichroic spectrum was then computed by subtracting the perpendicular polarized spectrum from the parallel one, as described previously. Before starting the deuteration, four spectra of the sample were recorded for each polarization to test the stability of the measurements. At zero time, the D<sub>2</sub>O-saturated N<sub>2</sub> flux, at a flow rate of 100 ml/min (controlled by a Brooks flow meter), was connected to the sample. For each kinetic time point, 24 scans were recorded and averaged at a resolution of 2 cm<sup>-1</sup> for each polarization.

The signal from the atmospheric water was subtracted from each spectrum [27]. Previous experiments have demonstrated that the dichroic spectrum of LmrA arises only from the oriented membrane helices [14], as the cytoplasmic domain possesses no specific orientation. In this case, the shift of the amide I dichroic spectrum during the time of exposure to D<sub>2</sub>O allowed us to evaluate specifically the exchange rate of the transmembrane helices. This shift occurred between 1658 cm<sup>-1</sup>, corresponding to the H form of  $\alpha$ -helices, and 1648 cm<sup>-1</sup>, corresponding to the D form of  $\alpha$ -helices [14].

### 2.6. ATP hydrolysis

ATPase activity was determined by measuring the release of inorganic phosphate (Pi) from ATP, using a colorimetric method adapted from [28]. The liberation of Pi was quantified after 1 h incubation of the samples (containing 1–2  $\mu$ g of LmrA reconstituted into liposomes, in the presence or absence of 10  $\mu$ M DNR) in the presence of 3 mM MgATP at 37°C. The effect of the free hydrolysis of MgATP and of DNR on the colorimetric assay was subtracted.

### 2.7. Tryptophan fluorescence quenching experiments

Acrylamide quenching experiments were carried out on an SLM Aminco 8000 fluorimeter at an excitation wavelength of 290 nm to reduce the absorbance of acrylamide. Acrylamide aliquots were added from a 3 M solution to the proteoliposome suspension containing 6.5  $\mu$ g of reconstituted LmrA and the various ligands. The final concentrations for DNR and nucleotides were 10  $\mu$ M and 3 mM, respectively. Tryptophan fluorescence intensities were measured at 332 nm after each addition of quencher. All measurements were carried out at room temperature. Control experiments established that no emission of DNR occurred at 332 nm if excited at 290 nm [29]. Acrylamide quenching data were analyzed according to the Stern–Volmer equation for collisional quenching [30]:

$$F_0/F = 1 + K[Q]$$

where  $F_0$  and  $F$  are the fluorescence intensities in the absence and presence of quencher,  $[Q]$  is the molar concentration of quencher, and  $K$  is the Stern–Volmer quenching constant. Data were subjected to a linear fit up to 80 mM acrylamide. Above this concentration, the static quenching by acrylamide causes a deviation from linearity in Stern–Volmer plots.

## 3. Results

### 3.1. Restructuring of the membrane-embedded domain of LmrA during its catalytic cycle

Polarized ATR-FTIR spectroscopy is one of the best tools available to characterize the structure (secondary structure and orientation) of the membrane-embedded domain of membrane proteins. The method is based on the fact that the infrared light absorbed by a chemical bond is maximal if its dipole transition moment is parallel to the electric field component of the incident light. By measuring the spectral intensity while turning the incident light electric field orientation with a polarizer, it is possible to obtain information about the orientation of the dipoles [23]. Orientation of secondary structures can be determined according to the orientation of the

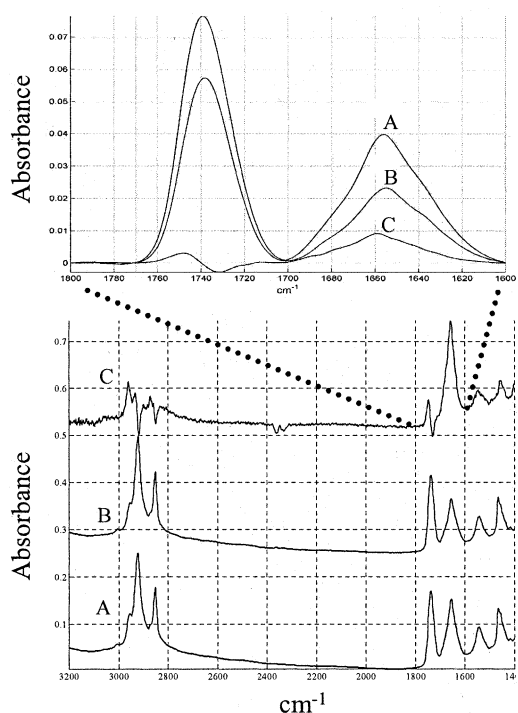


Fig. 1. Polarized infrared and dichroic spectra of LmrA. ATR-FTIR spectra of 20  $\mu$ g of LmrA recorded with incident light polarized parallel (A) or perpendicular (B) to the incident plane. The dichroic spectrum (C) is obtained by subtracting A from B. Spectrum C has been increased four-fold for clarity. Inset shows the superposition of these three spectra.

amide C=O dipole with respect to the membrane. Two spectra are recorded with the incident light polarized parallel and perpendicular with respect to the membrane plane. A qualitative analysis of the orientation of secondary structures with respect to the membrane is obtained by subtracting the  $\perp$  from the  $\parallel$  polarized spectrum. In the absence of any orientation, a straight horizontal line is expected in the amide I region of the dichroic spectrum [23]. Positive deviations indicate a transition dipole oriented close to perpendicular to the membrane, while negative deviations indicate a dipole alignment approximately in the membrane plane. For instance, a transmembrane  $\alpha$ -helix will give rise to a positive deviation as its amide I dipole is parallel to its long axis. The dichroic spectrum of LmrA shows an upward deviation at 1659 cm<sup>-1</sup>, characteristic of  $\alpha$ -helices perpendicular to the membrane [14] (Fig. 1). As confirmed by proteolysis studies, these helices compose the membrane-embedded domain of LmrA [14]. No specific orientation of the cytosolic domain of LmrA with respect to the membrane was detected. These observations demonstrated that only the transmembrane helices contribute significantly to the dichroism.

To characterize the ligand-induced restructuring of the membrane-embedded domain, we first analyzed the effect of drug binding and ATP hydrolysis on the main orientation of the transmembrane helices. Quantitative evaluation of the helix mean tilt requires the evaluation of the dichroic ratio  $R^{\text{ATR}}$  of amide I and of  $R^{\text{iso}}$ , which is the dichroic ratio measured for a transition dipole either spatially disordered or oriented at the magic angle [26]. As indicated in Section 2, and as developed in [26],  $R^{\text{iso}}$  is computed on the basis of the lipid

Table 1  
Dichroic ratio  $R^{\text{ATR}}$  of the amide I band of LmrA determined in the absence and presence of substrates

Substrate	Dichroic ratio	
	$R^{\text{iso}}$	$R^{\text{ATR}}$
None	1.5 $\pm$ 0.1	1.9 $\pm$ 0.1
+DNR	1.4 $\pm$ 0.1	1.9 $\pm$ 0.1
+DNR+MgATP $\gamma$ S	1.5 $\pm$ 0.1	1.8 $\pm$ 0.1
+DNR+MgATP	1.5 $\pm$ 0.1	1.9 $\pm$ 0.1

$R^{\text{ATR}}$  and  $R^{\text{iso}}$  (for the lipid  $\nu(\text{C}=\text{O})$ ) were calculated as described in Section 2.

ester band (between 1800 and 1700  $\text{cm}^{-1}$ , Fig. 1). We compared the dichroic ratio  $R^{\text{ATR}}$  obtained in the presence and absence of different ligands.  $R^{\text{ATR}} = 1.9 \pm 0.1$ , which corresponds to a main orientation of the helices perpendicular to the membrane (Table 1). Table 1 shows that  $R^{\text{ATR}}$  does not change significantly in the presence of DNR, MgATP $\gamma$ S or MgATP. With a standard deviation of 0.1 for the  $R^{\text{ATR}}$  determination, only changes in the helix tilt of more than  $3^\circ$  are detected. Consequently, the main tilt of the membrane-embedded helices seems unaffected upon drug or ATP binding or during ATP hydrolysis.

Although the mean tilt of the membrane helices is not modified upon interaction with substrates, rotation or translation of helices may modify their general packing. These conformational changes may affect their accessibility towards the external medium but also the strength of the H bonds stabilizing their structure, two parameters which affect H/D exchange kinetics [31]. While the amide II area decrease as a function of time can be used to evaluate the global exchange kinetic of the protein, the amide II band displays only low dichroism which makes it useless for the determination of the exchange kinetic of LmrA membrane-embedded helices [32]. In contrast, the maximum of the dichroism of amide I shifts between the H form of  $\alpha$ -helices (maximum at  $\sim 1658 \text{ cm}^{-1}$ ) and the D form (maximum at  $\sim 1648 \text{ cm}^{-1}$ ) during the time of exposure to  $\text{D}_2\text{O}$  (Fig. 2). Consequently, the stability and accessibility towards the external medium of the transmembrane segments of LmrA can be estimated by following the shift of the maximum of the dichroic amide I during the time of exposure to  $\text{D}_2\text{O}$ .

Fig. 3 shows that the dichroic amide I shift occurs between 1658 and 1652  $\text{cm}^{-1}$  in the protein alone. Binding of DNR mediates a slight modification of the amide I shift (from 1658  $\text{cm}^{-1}$  to 1653  $\text{cm}^{-1}$ ). It demonstrates that drug binding mediates a conformational change in the transmembrane helices.

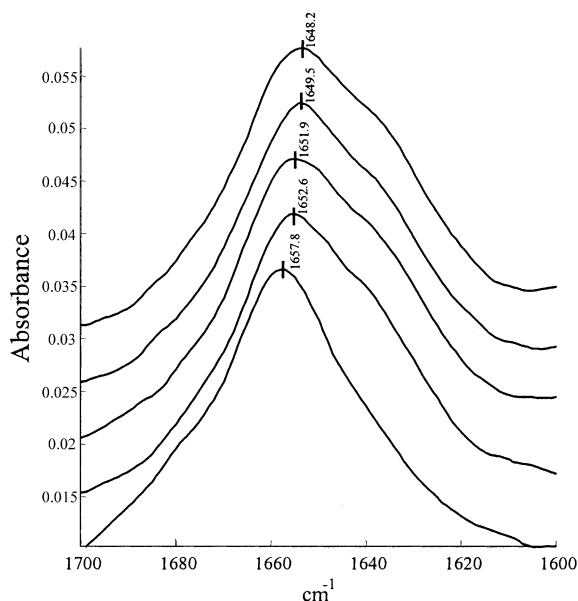


Fig. 2. Dichroic spectra of LmrA during the H/D exchange kinetics. Spectra of 20  $\mu\text{g}$  of LmrA recorded as a function of deuteration time. Spectrum at the bottom was recorded before deuteration. The other spectra were recorded at intermediate times (4, 11, 18, 42 min respectively).

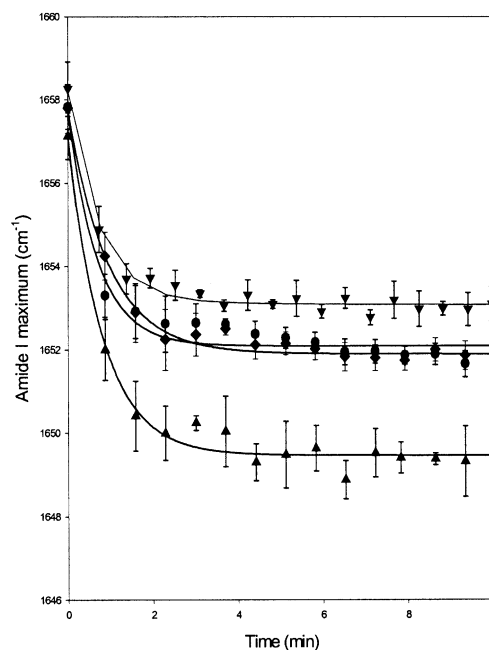


Fig. 3. Evolution of the amide I maximum of the dichroic spectrum as a function of the deuteration time. ●, no substrate added; ▼, DNR; ◆, MgATP $\gamma$ S+DNR; ▲, MgATP+DNR. The curves are the means of at least three experiments. The error bars represent the standard deviation.

The decrease of the amide I shift means that the packing of the transmembrane helices has changed in a way that leads to a higher strength of their H bonds, corresponding to a more rigid structure, or to a reduced accessibility towards the solvent of the  $\alpha$ -helices. In the presence of DNR and MgATP $\gamma$ S, the amide I shift is identical to that observed in the absence of ligand. We can reject the possibility that nothing happens when DNR and MgATP $\gamma$ S are added together. Indeed, an ATP-dependent drug transport is detectable in our sample [22], which means that DNR and ATP are able to bind simultaneously to LmrA. Furthermore, we have demonstrated that DNR and MgATP $\gamma$ S, added separately, induce a structural modification of LmrA (see [33] for the structural effect mediated by MgATP $\gamma$ S). Consequently, when added together, both structural effects must be observed. The amide I shifts in the presence of DNR alone or DNR/ATP $\gamma$ S are different, which means that a structural effect due to ATP binding is indeed observed on the transmembrane helices. The average stability and accessibility towards the solvent of the membrane-embedded domain is, however, equivalent to that before the interaction with ligands. Coaddition of DNR and MgATP causes an amide I shift from 1658  $\text{cm}^{-1}$  to 1649  $\text{cm}^{-1}$  revealing that the transmembrane helices undergo an important structural change that decreases the strength of their H bonds, corresponding to a more flexible structure, or increases their accessibility towards the external medium.

First, these results demonstrate that the transmembrane domain of LmrA is not static as it undergoes several conformational changes in the presence of ligands. Second, our observations provide evidence that ATP binding and hydrolysis mediate long-range conformational changes transmitted from the cytosolic NBD to the membrane-embedded domain of LmrA. Electron cryo-microscopy of two-dimensional crystals

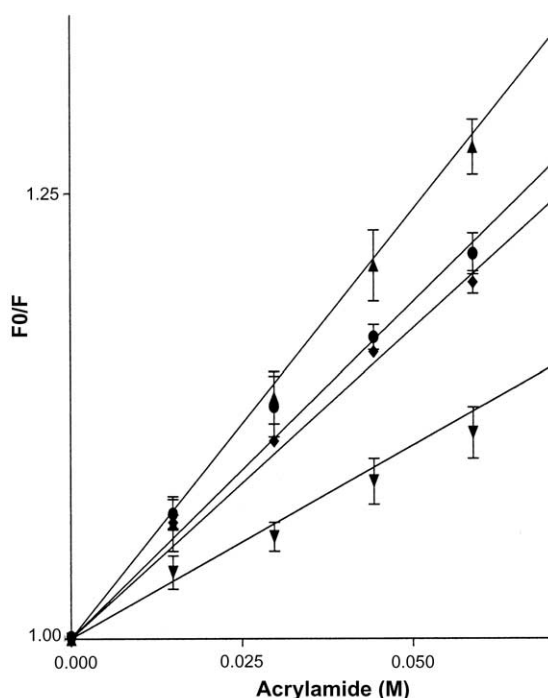


Fig. 4. Tryptophan quenching by acrylamide: Stern–Volmer plots.  $F$  is the measured fluorescence intensity and  $F_0$  is the fluorescence intensity in the absence of acrylamide. ●, no substrate added; ▼, DNR; ◆, MgATP $\gamma$ S+DNR; ▲, DNR+MgATP. The curves are the means of at least three experiments. The error bars represent the standard deviation.

of Pgp, the eukaryotic homologue of LmrA, have also demonstrated important repacking of its transmembrane  $\alpha$ -helices during the transport ATPase cycle [20]. The fact that the  $R^{\text{ATR}}$  of the transmembrane helices of LmrA is not modified in the presence of substrates means that the restructurings of the membrane-embedded domain do not modify the global tilt of the transmembrane helices. Consequently, rotation or translation movements of the  $\alpha$ -helices within the membrane may be involved in these restructurings of the membrane-embedded domain. Biochemical evidence of such rotation of transmembrane  $\alpha$ -helices of Pgp [20,34] and ions channels [35,36] has been previously reported.

### 3.2. Identification of restructuring occurring specifically in the cytosolic regions of LmrA during its catalytic cycle

LmrA contains five Trp residues, all predicted in extramembrane domains [6]. Two are located in cytoplasmic loops connecting helices 2 and 3 and helices 4 and 5. A third one is located in the extracellular loop connecting helices 3 and 4. Two others are located in the cytosolic loop following helix 6 and containing the NBD. As the protein is reconstituted in an inside-out configuration [14], only the four Trp localized in cytoplasmic loops are accessible to the aqueous quencher acrylamide. Consequently, the accessibility of these Trp to the aqueous medium makes it possible to investigate the behavior of the cytosolic regions of LmrA upon binding of DNR/ATP and during ATP hydrolysis. The Trp exposure to the external solvent was determined by monitoring the fluorescence intensity in the presence of increasing concentrations (0–80 mM) of the aqueous quencher acrylamide [37]. DNR was added to a

final concentration of 10  $\mu$ M to LmrA reconstituted into liposomes in the presence or absence of 3 mM MgATP or MgATP $\gamma$ S.

Stern–Volmer plots of Trp fluorescence quenching by acrylamide are shown in Fig. 4. DNR binding leads to a decreased accessibility of at least some Trp to the aqueous medium providing strong evidence that drug binding influences the structure of cytosolic regions of LmrA and that a conformational change is transmitted from the membrane-embedded  $\alpha$ -helices to the cytosolic domains. Upon coaddition of DNR and MgATP $\gamma$ S, the average Trp accessibility is similar to that observed in the absence of ligand. As discussed for H/D exchange experiments carried out in the presence of DNR and MgATP $\gamma$ S, we can reject the possibility that nothing happens in this situation and conclude that ATP binding affects the structure of some extramembrane segments of LmrA. Upon coaddition of MgATP and DNR, the accessibility of some Trp to the aqueous environment is strongly enhanced, demonstrating that some cytosolic segments become highly accessible to the aqueous environment.

To investigate whether the tertiary structure modification mediated by DNR binding in cytosolic segments of LmrA affects directly the ATPase activity of the NBD, ATP hydrolysis activity was measured in the presence of 10  $\mu$ M DNR. DNR binding stimulates the ATPase activity of reconstituted LmrA from  $200 \pm 20$  to  $300 \pm 20$  nmol/min/mg.

## 4. Discussion

Transport of drugs by LmrA implicates their extrusion from the membrane binding sites into the extracellular environment using the energy derived from ATP hydrolysis. Several conformational changes are likely to be involved in this process. Reorganization of the drug binding site, altering its exposure to the membrane or aqueous environment and its drug affinity, seems to be essential to facilitate drug binding and subsequent release. The existence of two cooperative drug binding sites on LmrA has been suggested in [11]: a low-affinity one on the outer membrane surface allosterically coupled to another site with high affinity on the inner membrane surface. The low-affinity outside-facing site seems only accessible in the ADP/vanadate-trapped LmrA suggesting that the conversion between these two sites depends on ATP hydrolysis [11]. X-ray crystallography of MsbA [15] also suggests that tertiary rearrangements of the transmembrane domain of MDR-ABC transporters mediated by the ATPase activity are implicated in their transport mechanism.

Our study provides evidence that the transmembrane segments of LmrA are not static during the transport cycle, as expected for a membrane transporter whose function requires conformational flexibility [11]. Previous experiments indicated that the H/D exchange of other membrane-embedded helices of integral membrane proteins, such as lactose permease [38] or the erythrocyte glucose transporter [39], is fast. Membrane-embedded helices of integral membrane proteins, such as bacteriorhodopsin [40], EmrE [41] and SliK [42], however, display slow exchange rates. How flexibility of membrane proteins is related to their biological function is still a matter of debate.

In a second step, we demonstrated that a structural coupling between the cytosolic and membrane-embedded domains of LmrA exists which probably allows the cross-talk between the ATPase activity in the cytosolic NBD and drug

transport from the lipid bilayer to the external medium. Indeed, on the one hand, the membrane-embedded domain of LmrA undergoes dynamic changes mediated by the ATPase activity. These changes do not modify the mean tilt of the transmembrane helices and consequently may be due to their rotation or translation. Rotation may indeed explain how the substrate binding site of LmrA can be alternately exposed to the lipid phase and then the aqueous phase before the drug is released to the extracellular medium. A restructuring of the transmembrane  $\alpha$ -helices of Pgp during the ATPase cycle has also been observed on two-dimensional crystals and by using cross-linking experiments [20,34]. A rotational model was also proposed to explain these data. We observed that the ATPase activity of LmrA mediates at least two distinct restructurings of the membrane-embedded  $\alpha$ -helices, one due to ATP binding and another due to ATP hydrolysis. A similar conclusion was reached from two-dimensional crystals of Pgp [20]. Rosenberg et al. proposed in [20] that ATP binding in the NBD induces a major conformational change reducing the affinity for substrate. This hypothesis is corroborated by radioligand binding assay [43]. They further suggested that after ATP binding, the drug binding site is reoriented towards the external medium. We observed that H/D exchange kinetics of LmrA are similar before and after ATP binding. This seems to be in contradiction with the opening of a large chamber towards the external medium. ATP hydrolysis, however, mediates a drastic change in the H/D exchange kinetics of the transmembrane segments. Consequently, we propose that if ATP binding induces a decrease in drug affinity, ATP hydrolysis mediates the reorientation of the drug binding site towards the external medium. Similar conclusions were obtained from ATR-FTIR experiments on Pgp [44].

We also demonstrated that the cytosolic regions of LmrA, containing the NBD and loops, undergo conformational changes during the transport process. First, DNR binding affects the accessibility of these cytosolic segments to the aqueous environment. It is likely that DNR-mediated stimulation of the ATPase activity is related to this conformational modification. These observations demonstrate that the cross-talk between the membrane-embedded and cytosolic regions occurs in both directions. Moreover, ATP binding and hydrolysis increase the accessibility towards the solvent of some cytosolic regions of LmrA. Several experiments including the crystal structure determination of the ATP binding domain of HisP [15] and fluorescence measurements on Pgp [45,46] have demonstrated that the NBD domain of ABC proteins is highly apolar and it is likely that the NBD of LmrA is mainly organized as a hydrophobic pocket. Consequently, the highly accessible conformation reached by some cytosolic segments of LmrA in the presence of nucleotides probably does not involve the NBD itself but some cytosolic loops. We deduce that some intracellular loops may function as a conduit coupling ATP hydrolysis by NBD to tertiary rearrangements of the flexible transmembrane helices.

## References

- [1] Nikaido, H. (1994) *Science* 264, 382–388.
- [2] Gottesman, M.M. (1993) *Cancer Res.* 53, 747–754.
- [3] Endicott, J.A. and Ling, V. (1989) *Annu. Rev. Biochem.* 58, 137–171.
- [4] Cole, S.P., Bhardwaj, G., Gerlach, J.H., Mackie, J.E., Grant, C.E., Almquist, K.C., Stewart, A.J., Kurz, E.U., Duncan, A.M. and Deeley, R.G. (1992) *Science* 258, 1650–1654.
- [5] Putman, M., van Veen, H.W. and Konings, W.N. (2000) *Microbiol. Mol. Biol. Rev.* 64, 672–693.
- [6] van Veen, H.W., Venema, K., Bolhuis, H., Oussenko, I., Kok, J., Poolman, B., Driessen, A.J. and Konings, W.N. (1996) *Proc. Natl. Acad. Sci. USA* 93, 10668–10672.
- [7] van Veen, H.W., Callaghan, R., Soceneantu, L., Sardini, A., Konings, W.N. and Higgins, C.F. (1998) *Nature* 391, 291–295.
- [8] Higgins, C.F. (1992) *Annu. Rev. Cell Biol.* 8, 67–113.
- [9] Gros, P., Croop, J. and Housman, D. (1986) *Cell* 47, 371–380.
- [10] Chen, C.J., Chin, J.E., Ueda, K., Clark, D.P., Pastan, I., Gottesman, M.M. and Roninson, I.B. (1986) *Cell* 47, 381–389.
- [11] van Veen, H.W., Margolles, A., Muller, M., Higgins, C.F. and Konings, W.N. (2000) *EMBO J.* 19, 2503–2514.
- [12] Bolhuis, H., van Veen, H.W., Molenaar, D., Poolman, B., Driessen, A.J. and Konings, W.N. (1996) *EMBO J.* 15, 4239–4245.
- [13] Loo, T.W. and Clarke, D.M. (1999) *J. Biol. Chem.* 274, 24759–24765.
- [14] Grimard, V., Vigano, C., Margolles, A., Wattiez, R., van Veen, H.W., Konings, W.N., Ruyschaert, J.M. and Goormaghtigh, E. (2001) *Biochemistry* 40, 11876–11886.
- [15] Chang, G. and Roth, C.B. (2001) *Science* 293, 1793–1800.
- [16] Locher, K.P., Lee, A.T. and Rees, D.C. (2002) *Science* 296, 1091–1098.
- [17] Ramachandra, M., Ambudkar, S.V., Chen, D., Hrycyna, C.A., Dey, S., Gottesman, M.M. and Pastan, I. (1998) *Biochemistry* 37, 5010–5019.
- [18] Sauna, Z.E. and Ambudkar, S.V. (2000) *Proc. Natl. Acad. Sci. USA* 97, 2515–2520.
- [19] Martin, C., Berridge, G., Mistry, P., Higgins, C., Charlton, P. and Callaghan, R. (2000) *Biochemistry* 39, 11901–11906.
- [20] Rosenberg, M.F., Velarde, G., Ford, R.C., Martin, C., Berridge, G., Kerr, I.D., Callaghan, R., Schmidlin, A., Wooding, C., Linton, K.J. and Higgins, C.F. (2001) *EMBO J.* 20, 5615–5625.
- [21] Urbatsch, I.L., Marwan, K., Al-Shawi, K. and Senior, A.E. (1994) *Biochemistry* 33, 7069–7076.
- [22] Margolles, A., Putman, M., van Veen, H.W. and Konings, W.N. (1999) *Biochemistry* 38, 16298–16306.
- [23] Goormaghtigh, E., Raussens, V. and Ruyschaert, J.M. (1999) *Biochim. Biophys. Acta* 1422, 105–185.
- [24] Fringeli, U. and Günthard, H. (1981) *Mol. Biol. Biochem. Biophys.* 31, 270–332.
- [25] Goormaghtigh, E. and Ruyschaert, J.M. (1990) in: *Molecular Description of Biological Membranes by Computer Aided Conformational Analysis* (Brasseur, R., Ed.), pp. 285–329, CRC Press, Boca Raton, FL.
- [26] Bechinger, B., Ruyschaert, J.M. and Goormaghtigh, E. (1999) *Biophys. J.* 76, 552–563.
- [27] Goormaghtigh, E., de Jongh, H.H. and Ruyschaert, J.M. (1996) *Appl. Spectrosc.* 50, 1519–1527.
- [28] Chifflet, S., Torriglia, A., Chiesa, R. and Tolosa, S. (1988) *Anal. Biochem.* 168, 1–4.
- [29] Ferrer-Montiel, A.V., Gonzalez-Ros, J.M. and Ferragut, J.A. (1988) *Biochim. Biophys. Acta* 937, 379–386.
- [30] Lehrer, S.S. (1971) *Biochemistry* 10, 3254–3263.
- [31] Goormaghtigh, E., Cabiaux, V. and Ruyschaert, J.M. (1994) *Subcell. Biochem.* 23, 329–362.
- [32] Goormaghtigh, E., Cabiaux, V. and Ruyschaert, J.M. (1994) *Subcell. Biochem.* 23, 405–450.
- [33] Vigano, C., Margolles, A., van Veen, H.W., Konings, W.N. and Ruyschaert, J.M. (2000) *J. Biol. Chem.* 275, 10962–10967.
- [34] Loo, T.W. and Clarke, D.M. (2000) *J. Biol. Chem.* 275, 5253–5256.
- [35] Minor, D.L., Lin, Y.F., Mobley, B.C., Avelar, A., Jan, Y.N. and Berger, J.M. (2000) *Cell* 102, 657–670.
- [36] Cha, A., Snyder, G.E., Selvin, P.R. and Bezanilla, F. (1999) *Nature* 402, 809–813.
- [37] Eftink, M.R. and Ghiron, C.A. (1981) *Anal. Biochem.* 114, 199–227.
- [38] le Coutre, J., Narasimhan, L.R., Patel, C.K. and Kaback, H.R. (1997) *Proc. Natl. Acad. Sci. USA* 94, 10167–10171.

- [39] Alvarez, J., Lee, D.C., Baldwin, S.A. and Chapman, D. (1987) *J. Biol. Chem.* 262, 3502–3509.
- [40] Downer, N.W., Bruchman, T.J. and Hazzard, J.H. (1986) *J. Biol. Chem.* 261, 3640–3647.
- [41] Arkin, I.T., Russ, W.P., Lebediker, M. and Schuldiner, S. (1996) *Biochemistry* 35, 7233–7238.
- [42] le Coutre, J., Kaback, H.R., Patel, C.K., Heginbotham, L. and Miller, C. (1998) *Proc. Natl. Acad. Sci. USA* 95, 6114–6117.
- [43] Martin, C., Higgins, C.F. and Callaghan, R. (2001) *Biochemistry* 40, 15733–15742.
- [44] Vigano, C., Julien, M., Carrier, I., Gros, P. and Ruyschaert, J.M. (2002) *J. Biol. Chem.* 277, 5008–5016.
- [45] Baubichon-Cortay, H., Baggetto, L.G., Dayan, G. and Di Pietro, A. (1994) *J. Biol. Chem.* 269, 22983–22989.
- [46] Liu, R. and Sharom, F.J. (1996) *Biochemistry* 35, 11865–11873.